Supporting Information

MXene Hybrid Nanocomposites Enables Highly Performance Memory Devices and Artificial Synapse Applications

Cui Wang,[a],[b] Nuoya Li,[b] Hang Zeng,[a] Li Chen,*[a],[b] Di Wu,[a],[b] and Jianlong Xia*[a],[b]

[a] State Key Laboratory of Advanced Technology for Materials Synthesis and Processing, Center of Smart Materials and Devices, Wuhan University of Technology, No. 122 Luoshi Road, Wuhan 430070, China.

[b] School of Chemistry, Chemical Engineering and Life Science, Wuhan University of Technology, No. 122 Luoshi Road, Wuhan, 430070, China.

E-mail: J. L. Xia. (jlxia@whut.edu.cn); L. Chen. (lichen0430@whut.edu.cn)

The synthesis and characterization of Ti_3C_2Tx MXene

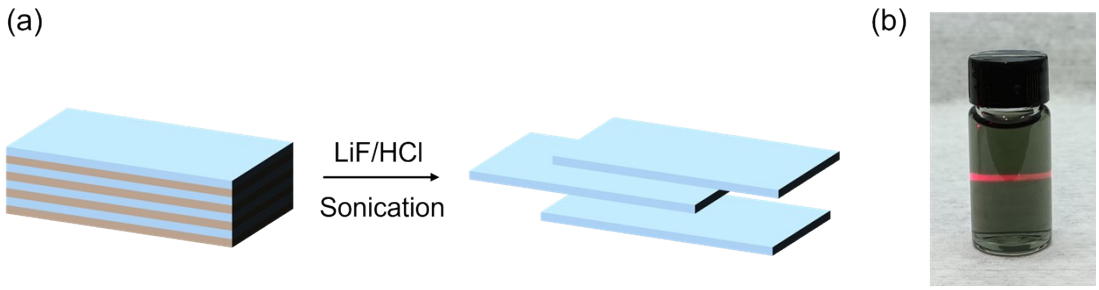

Figure S1. (a) Preparation of the MXene nanosheets, (b) Tyndall effect of the MXene nanosheets aqueous solution.

Synthesis of monomer 4-trifluoromethyl styrene

To a mixture of methyltriphenylphosphonium bromide (PPh_3MeBr, 10 mmol, 4.2 g) and THF (50 mL) was added into the two-necked flask, then add NaH (12 mmol, 280 mg) at room temperature and stir for 30 minutes under nitrogen atmosphere of 0 ℃. Then, add p-trifluoromethylbenzaldehyde (10 mmol, 1.7 g) slowly at 0 ℃ and stir at room temperature for 8 h. The reaction is quenched with water and extracted with DCM. Dry the organic phase with anhydrous $NaSO_4$ and concentrated under reduced pressure to afford the crude product, which was separated and purified by silica gel column chromatography (PE). The final product was obtained (yield 60%). ^{1}H NMR (500 MHz, Chloroform-*d*): δ 7.58 (d, *J* = 8.0 Hz, 2H), 7.50 (d, *J* = 8.0 Hz, 2H), 6.75 (dd, *J* = 17.6, 10.9 Hz, 1H), 5.85 (d, *J* = 17.6 Hz, 1H), 5.39 (d, *J* = 10.9 Hz, 1H)

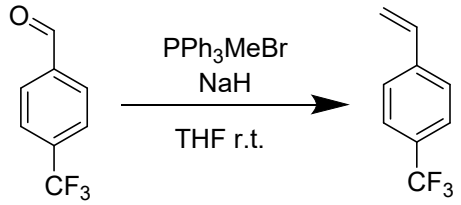

Figure S2. Synthetic route of 4-trifluoromethylstyrene.

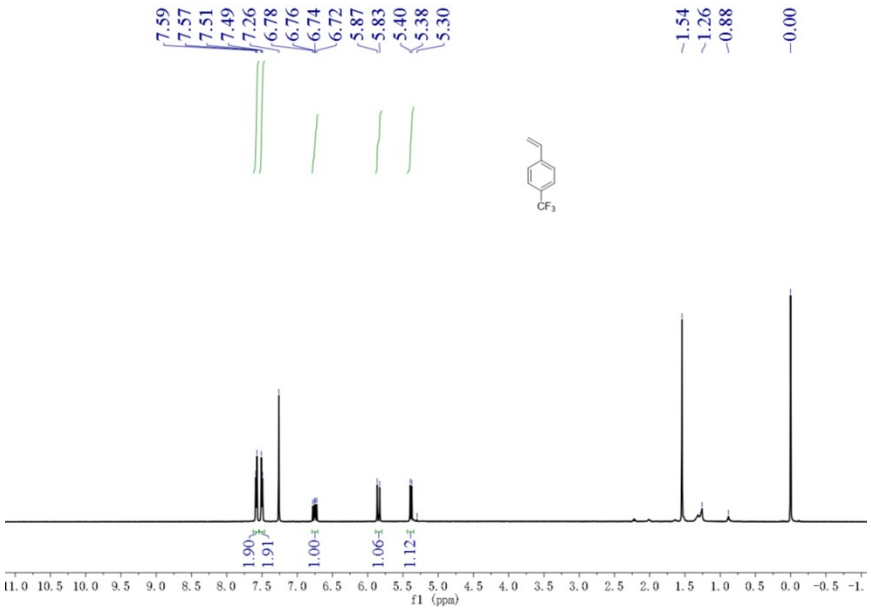

Figure S3. ^{1}H NMR spectroscopy of 4-trifluoromethylstyrene.

Synthesis of polymer 4-trifluoromethyl styrene (PTF)

To a mixture of monomer 4-trifluoromethyl styrene (2.46 mmol, 424 mg) and initiator azodiisobutyronitrile (AIBN, 0.1wt%) was added into a glass ampoule bottle. The mixture was stirred at 65 ℃ for 1 h and then heated at 80 ℃ for 24 hours under vacuum seal the ampoule bottle after three times of low-temperature freezing and air extraction cycles. The crude product is dissolved in chloroform and precipitated in methanol. The filtered final product was dried in a vacuum oven at 80 ℃ for 1 day, and the yield was 86%. ^{1}H NMR (500 MHz, Acetone-d_6): δ 7.05 (4H), 1.68 (3H). GPC data: $M_n = 1.16 \times 10^6$, PDI = 2.64.

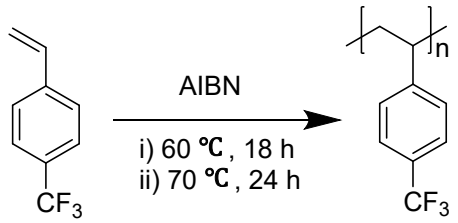

Figure S4. Synthetic route of PTF.

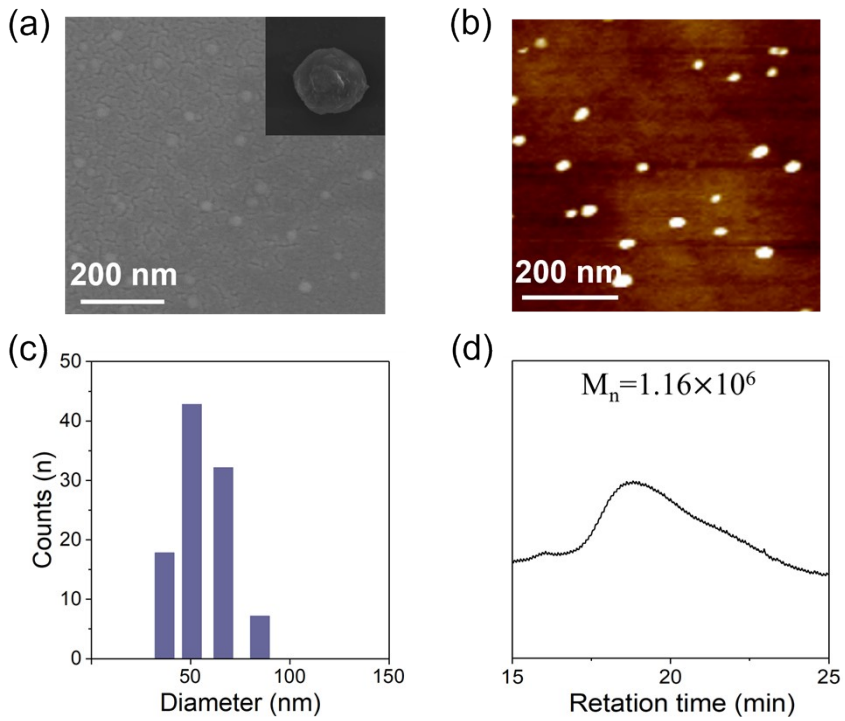

Figure S5. (a) SEM, (b) AFM, (c) Lateral size distribution and (d) GPC of PTF nanoparticles.

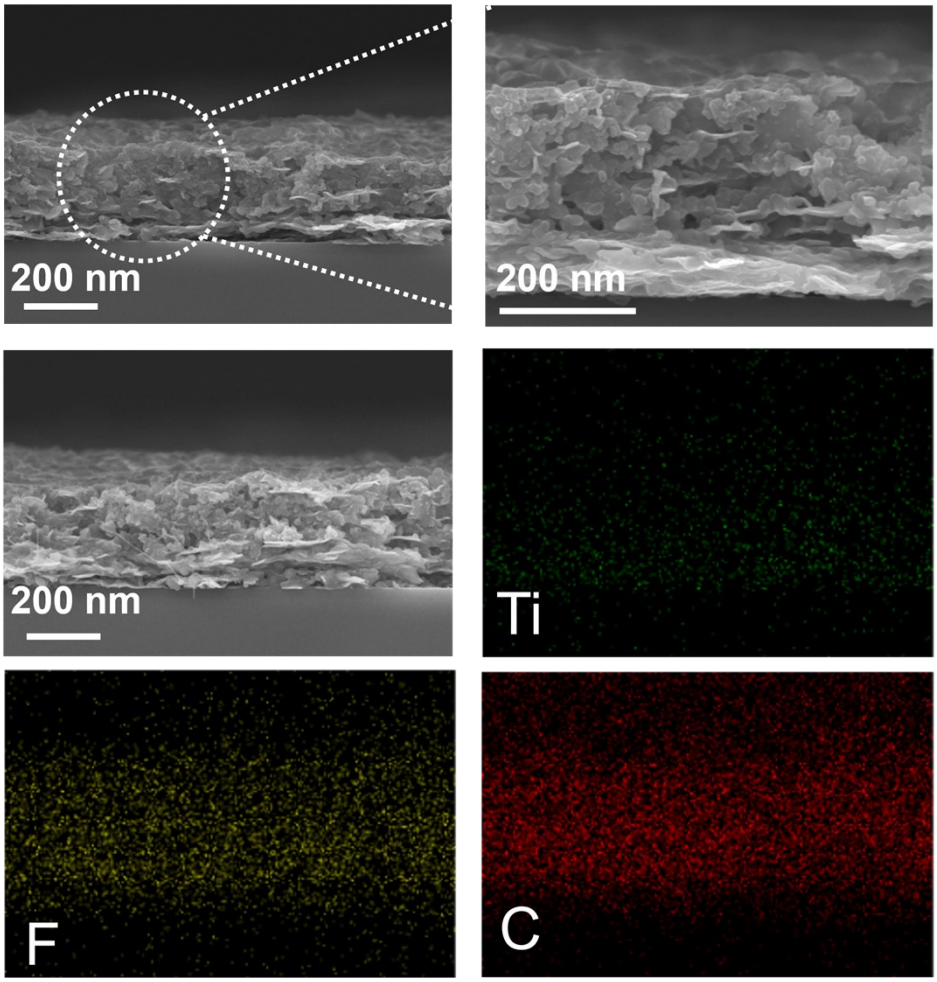

Figure S6. Crossing-SEM and EDXS images of MXP nanocomposite.

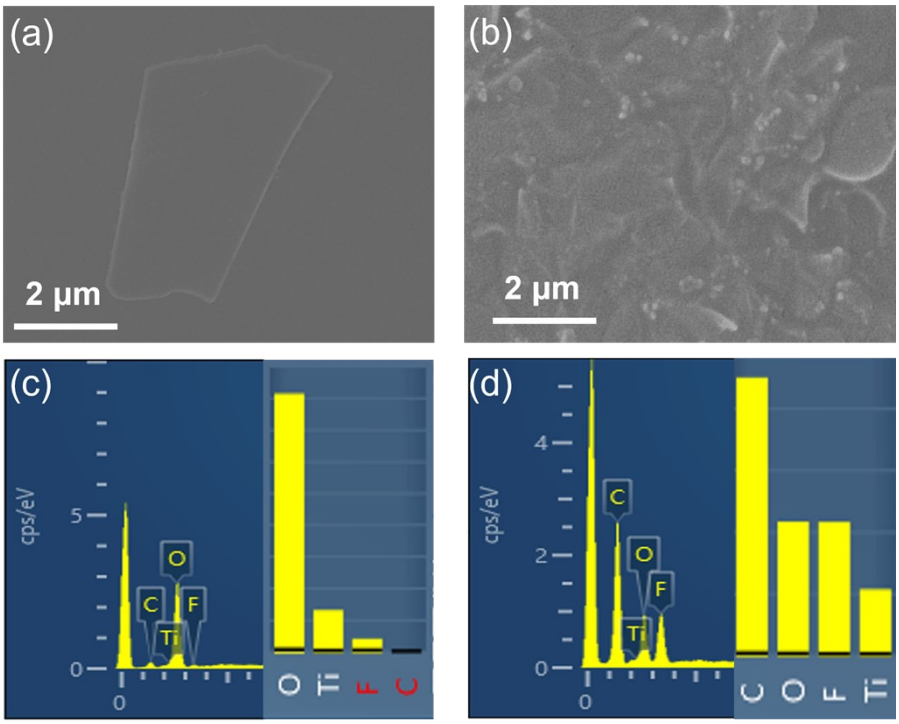

Figure S7. SEM image of a) MXene nanosheet, b) MXP nanocomposite, and mapping of element content distribution of c) MXene nanosheet, d) MXP nanocomposite.

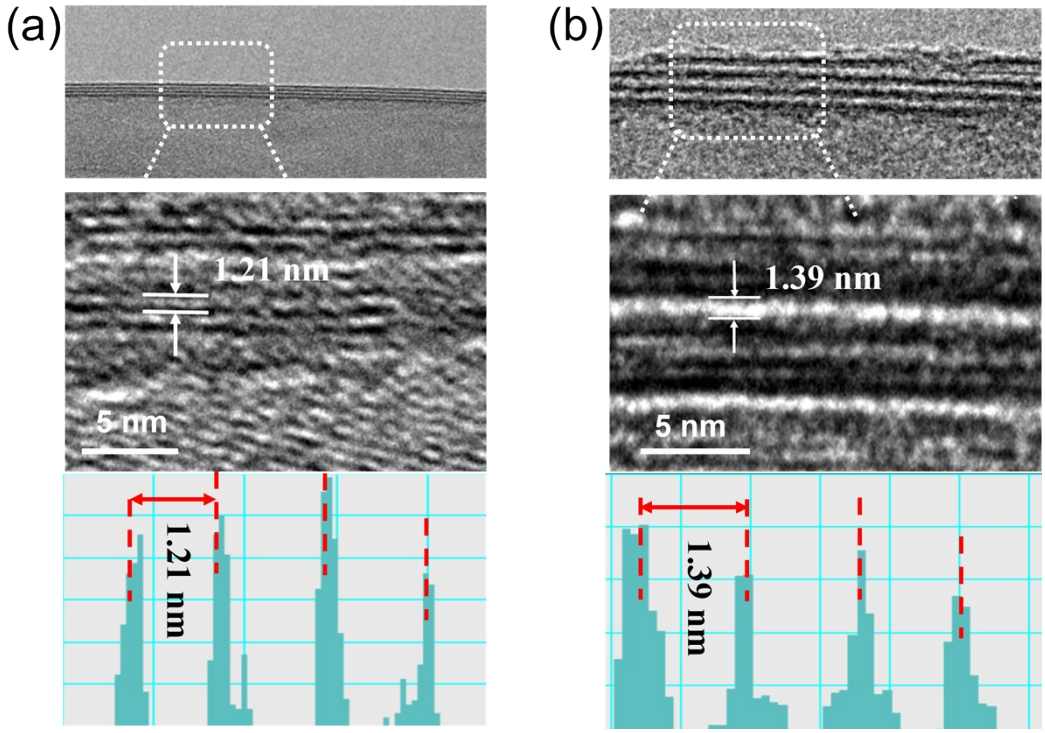

Figure S8. HRTEM images of a) MXene nanosheet, b) MXP nanocomposite, and the corresponding enlarged images.

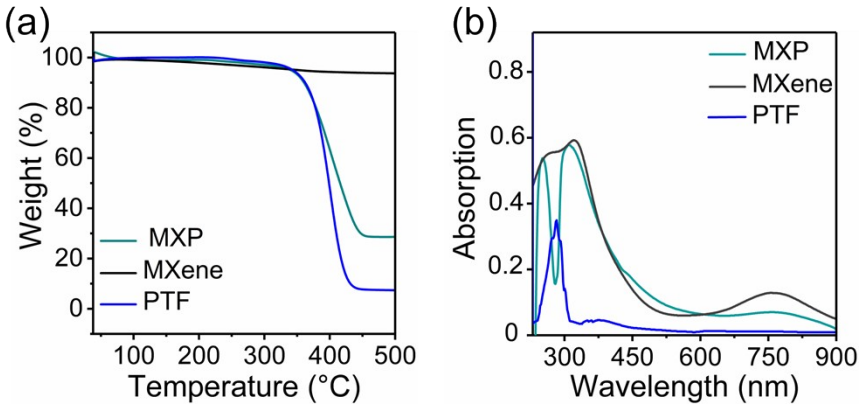

Figure S9. a) TGA curve and b) UV-Vis spectra of the PTF, MXene nanosheets and MXP nanocomposite.

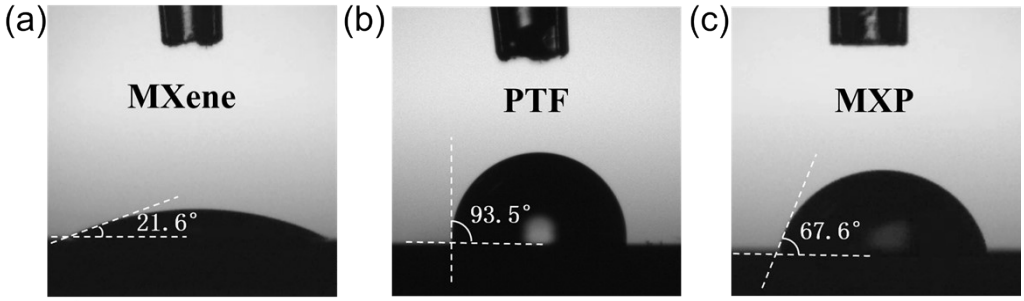

Figure S10. The contact angles of a) MXene nanosheets, b) PTF and c) MXP nanocomposite.

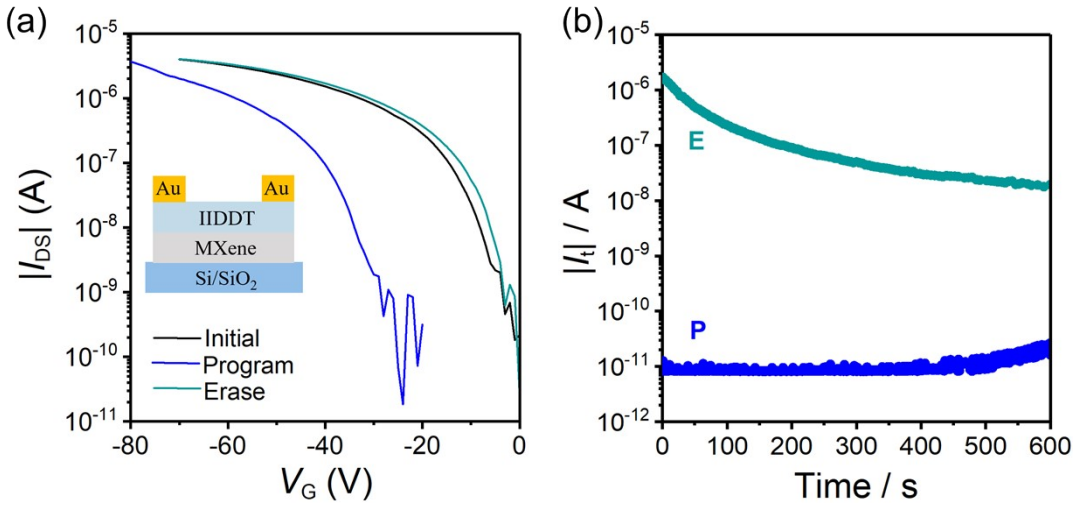

Figure S11. a) The programming and erasing characteristics of the memory with the MXene nanosheets as the floating gate under a negative programming gate voltage of −30 V for 10 s, b) the retention characteristics of the memory device. (P and E represent "programmed" and "erased," respectively).

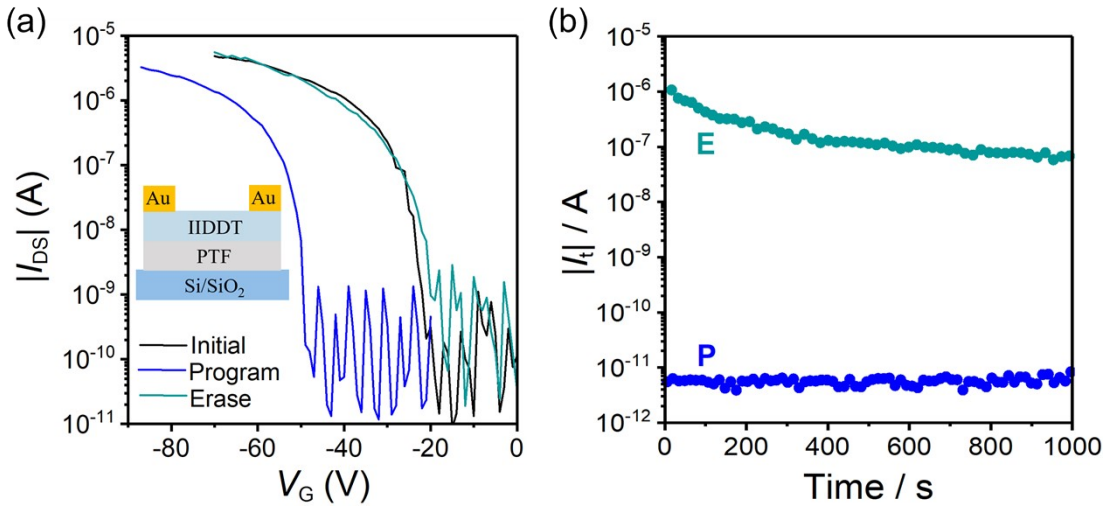

Figure S12. a) The programming and erasing characteristics of the memory with the PTF nanoparticles as the floating gate under a negative programming gate voltage of −30 V for 10 s, b) the retention characteristics of the memory device. (P and E represent "programmed" and "erased," respectively).

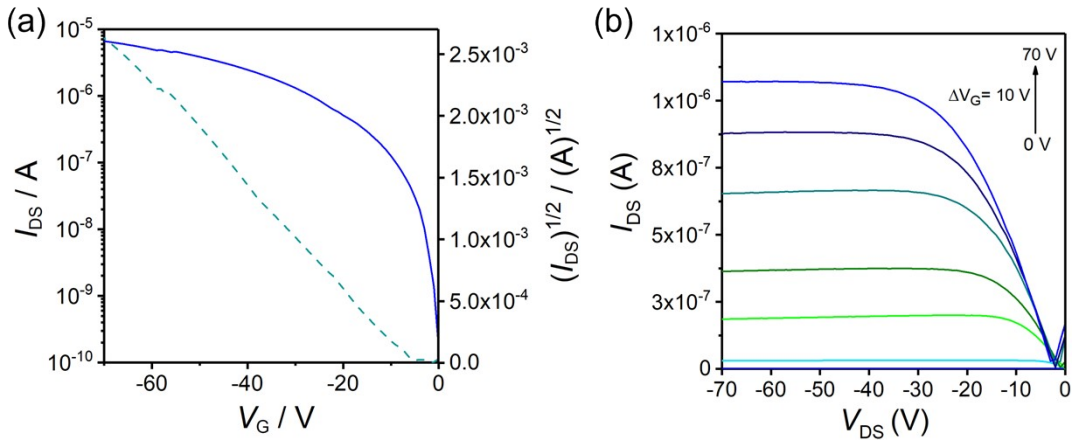

Figure S13. (a) Typical transfer and (b) Output characteristics of the memory devices.

(V_G = −70 V, V_{DS} = −70 V).

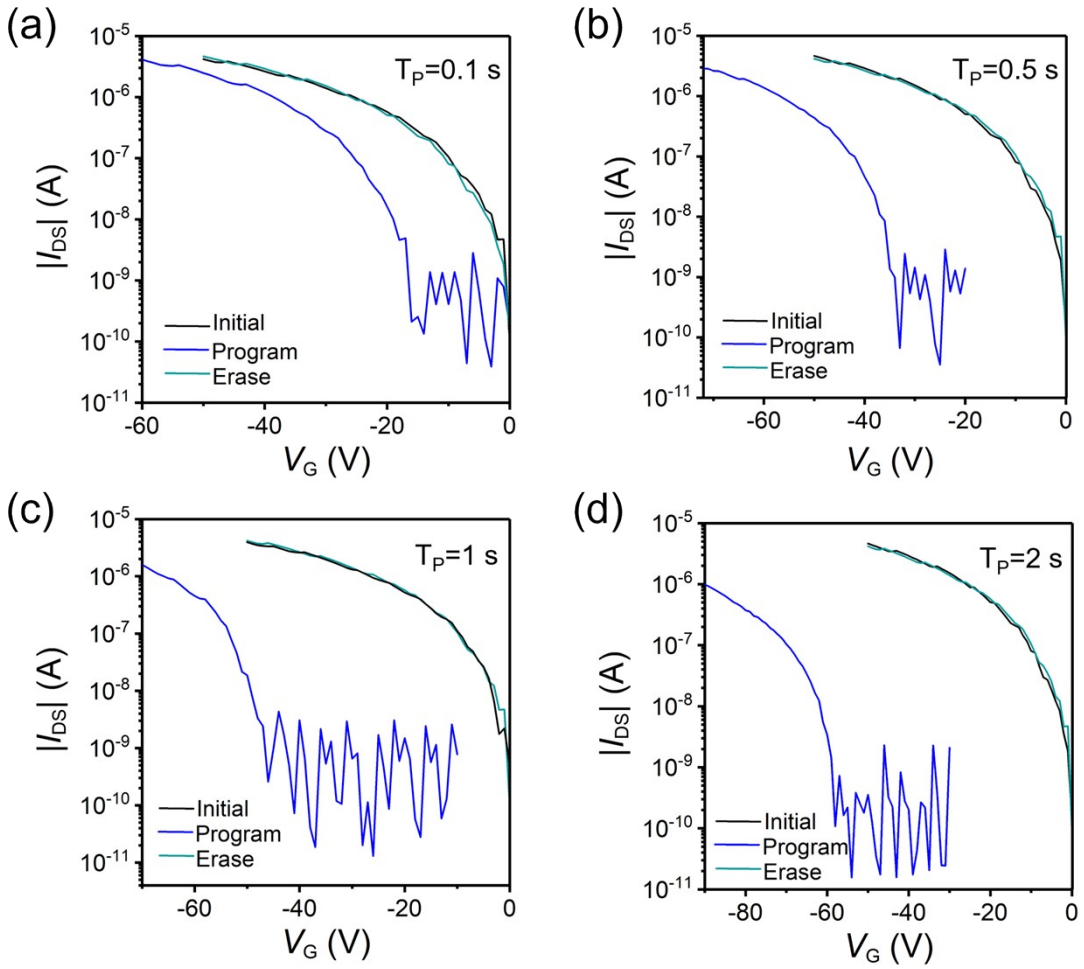

Figure S14. The typical transfer characteristics of the memory device in different program times in a) T_p = 0.1 s, b) T_p = 0.5 s, c) T_p = 1 s, d) T_p = 2 s.

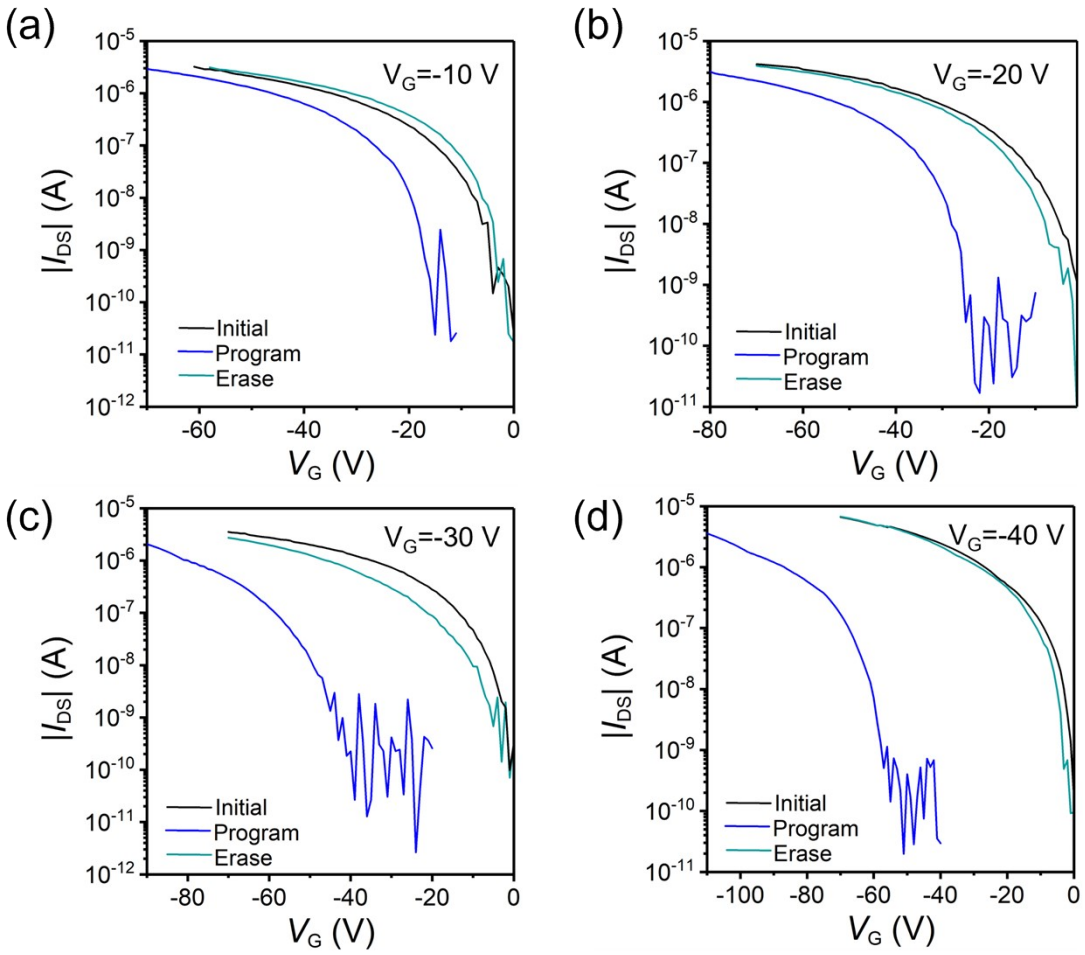

Figure S15. The typical transfer characteristics of the memory device in different V_G sweep at a) $V_G = -10$ V, b) $V_G = -20$ V, c) $V_G = -30$ V, d) $V_G = -40$ V.

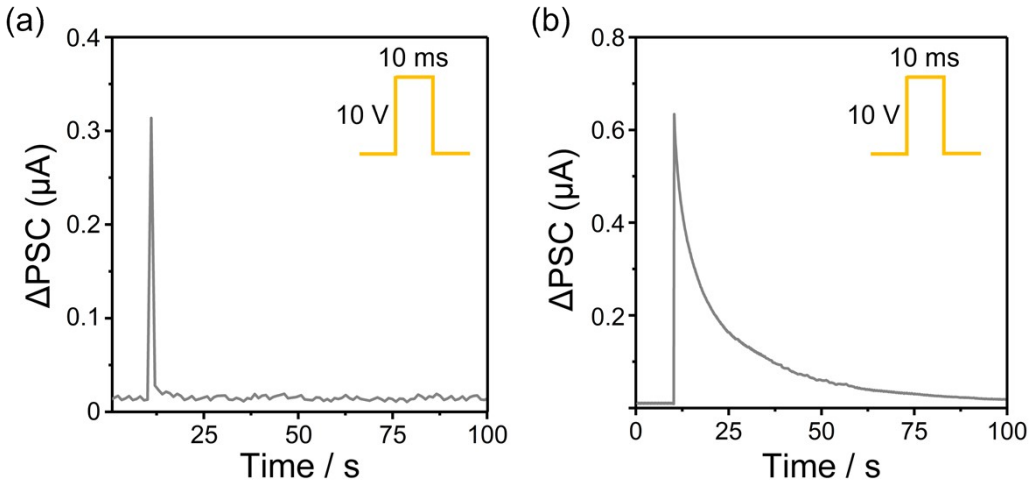

Figure S16. EPSC responses of memory device (a) with PTF nanoparticles as the floating gate (b) with the MXene nanosheets as the floating gate, to V_{WC} spike with magnitude of ±10 V and duration (t_d) of 10 ms.

Table S1. Comparisons with other floating gate materials.

Floating gate	Device type	Program/Erase voltage (V)	ΔV_T (V)	Retention time (s)	Endurance cycle	Synapse performance		Ref.
						V_{WC}(V)	Functions	
FPS	FET	±100	108	10^4	--		--	S1
PS+n-PyDI	FET	±120	35	10^4	400		--	S2
4-CF_3-PS	FET	±70	35	3×10^2	--		--	S3
MXene	FET	±50	35.2	10^4	10^3	±0.2	EPSC, IPSC, PPF, LTD, LTP	S4
MXene/Ion-gel	FET	±4	2	10^5	100	±10	IPSC, PPD, LTD, LTP	S5
MOF	FET	±80	37.5	10^4	100		--	S6
Ag@SiO_2	FET	±80	24	10^4	100		--	S7
AuNPs@PS	FET	±100	40	10^5	30		--	S8
GO/pyridinium/GO	Memristor	±5	--	10^3	10^3	±5	PPF, STP, EPSC, PPI, STDP, SRDP	S9
Ti_3C_2Tx-PVP	Memristor	±0.9	--	8×10^3	40		--	S10
PCBM−MoS_2	Memristor	±6	--	10^4	100		--	S11
MXP	FET	±40	47.8	10^5	10^4	±10	EPSC, IPSC, PPF, LTD, LTP	This work

ΔV_T represent the memory window, V_{WC} represent the weight control voltage pulses.

References

S1. Y-W. Zhu, Y-K. Fan, S-T. Li, P. Wei, D-F. Li, B. Liu, D-M. Cui, Z-C. Zhang, G-C. Li, Y-J. Niee and G-H Lu, *Mater. Horiz.*, **2020**, *7*, 1861.

S2. W-V. Wang, Y-M. Zhang, X-Y. Li, Z-Z. Chen, Z-H. Wu, L. Zhang, Z-W. Lin and H-L. Zhang, *InfoMat*, **2021**, *3*, 814–822.

S3. E. Plunkett, T. S. Kale, Q. Zhang, H. E. Katz and D. H. Reich, *Appl. Phys. Lett.*, 2019, **114**, 023301.

S4. B. Lyu, Y. Choi, H. Jing, C. Qian, H. Kang, S. Lee and J. H. Cho, *Adv. Mater.*, 2020, **32**, 1907633.

S5. S. Kim, S-B. Jo, J. Kim, D. Rhee, Y-Y. Choi, D-H. Kim, J. Kang and J. H. Cho, *Adv. Funct. Mater*. **2022**, *32*, 2111956.

S6. N. Shi, J. Zhang, Z. Ding, H. Jiang, Y. Yan, D. Gu, W. Li, M. Yi, F. Huang, S. Chen, L. Xie, Y. Ren, Y. Li and W. Huang, *Adv. Funct. Mater.*, 2022, **32**, 2110784.

S7. X. Guo, W. Zhang, J. Yin, Y. Xu, Y. Bai and J. Yang, *Org. Electron.*, 2021, **93**, 106149.

S8. K. Wang, H. Ling, Y. Bao, M. Yang, Y. Yang, M. Hussain, H. Wang, L. Zhang, L. Xie, M. Yi, W. Huang, X. Xie and J. Zhu, *Adv. Mater.*, 2018, **30**, 1800595.

S9. Y. Li, S-T. Ling, R-Y. He, C. Zhang, Y. Dong, C-L. Ma, Y-C. Jiang, J. Gao, J-H. He and Q-C Zhang, *Nano Res*., **2023**, *16*, 11278–11287.

S10. C. Gu, H. W. Mao, W. Q. Tao, Z. Zhou, X. J. Wang, P. Tan, S. Cheng, W. Huang, L.-B. Sun, X.-Q. Liu and J.-Q. Liu, A*CS Appl. Mater. Interfaces*, 2019, **11**, 38061-38067.

S11. W. Lv, H. Wang, L. Jia, X. Tang, C. Lin, L. Yuwen, L. Wang, W. Huang and R. Chen, A*CS Appl. Mater. Interfaces*, 2018, **10**, 6552-6559.